

Combining Mesenchymal Stem Cells Derived from Wharton's Jelly and Amniotic Biomaterial Scaffolds for Cell Delivery

Umamagesh Palaniappan, Jaianand Kannaiyan, Balaji Paulraj, Ponmurugan Karuppiah, Santhosh Basavarajappa, Asad Syed, Abdallah M. Elgorban, Nouf S. Zaghloul, and Veeramani Veeramanikandan*



Cite This: *ACS Omega* 2023, 8, 24351–24361



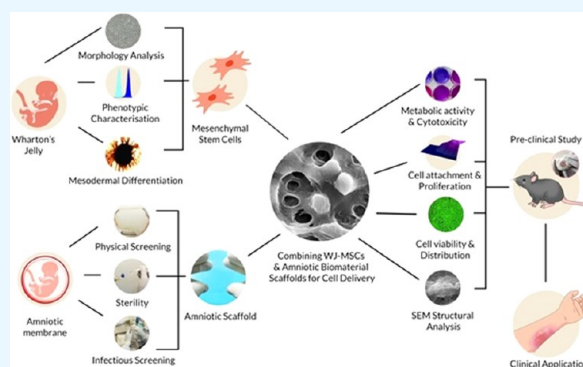
Read Online

ACCESS |

Metrics & More

Article Recommendations

ABSTRACT: Therapies based on mesenchymal stem cells have incredible potential for tissue regeneration. Tracking cells and keeping them at the injury site are creating challenges. The cells can be sown into a biocompatible scaffold as a possible remedy. Tissue engineering construction is a difficult, multistep process that requires many variables to be optimized, including the stem cell source, molecular components, scaffold architecture, and a suitable *in vivo* animal model. In order to locate a suitable regenerative scaffold for delivering stromal cells to regions with greater healing potential, we assessed whether human Wharton's Jelly-derived mesenchymal stem cells (WJMSCs) responded on biological membranes. WJMSCs were isolated, characterized, and seeded onto an amniotic membrane-based scaffold. Results obtained *in vitro* revealed that the seeded scaffolds had a significant impact on a number of critical variables, including seeding effectiveness, cellular dispersion, adhesion, survival, and metabolic activity. The research sheds light on a fresh facet of material behavior and paves the way for the creation of scaffold materials that support tissue regeneration and repair. Furthermore, the methods used herein can be utilized to test other scaffold materials to increase their healing potential with WJMSCs.



INTRODUCTION

Scaffolds are classified as biological (natural) or synthetic. Biological scaffolds originating from both human and animal tissues include human amniotic membrane (hAM), chitosan, hyaluronic acid, and cellulose, whereas synthetic scaffolds include hydroxyapatite (HA), tricalcium phosphate, poly(glycolic acid), and poly(lactic acid).^{1,2} Biological scaffolds are widely obtainable and are hence less costlier than synthetic scaffolds.² Furthermore, biological scaffolds give unique cell interaction, biocompatibility, and tissue-like characteristics that are largely adopted by host tissues.³ Chitosan is biocompatible, can be degraded by human enzymes, and is commonly utilized in natural scaffolds. However, it is frequently mixed with other bioactive compounds.⁴ Because it is readily accessible and very affordable, the amniotic membrane has evolved from the traditional substrate for bioengineering.

Amniotic membrane grafting has been routinely employed in wound care and other therapeutic approaches for more than a decade. There are two possible ways to implant an amniotic membrane: either as a stable graft that serves as a substrate for cells to develop or as a transient bandage or overlay that serves as a barrier.^{5,6} Because of its unique features, including reducing scarring, anti-inflammation effects, and enhancing

epithelialization, the amniotic membrane has grown in favor of wound-healing therapies. Several clinical investigations described the potential of amniotic membranes for tissue engineering in our earlier publication.^{5,7}

The amniotic membrane graft as a biological allograft can create a pathophysiological milieu similar to that of the autografts, creating an *in vivo* setting conducive to skin regeneration.^{1,5} On the other hand, to date, mesenchymal stem cells (MSCs) therapy has undoubtedly shown a favorable safety profile.^{8–10} Therefore, to employ the promising approaches in tissue engineering, combining mesenchymal stem cells (MSCs), and biomaterial scaffolds for successful cell delivery, new approaches are investigated.

The mechanical strengths of the basement membrane, as well as cell attachment and survival, of the biological allograft were evaluated in detail. The amniotic membrane (AM) has

Received: March 15, 2023

Accepted: June 9, 2023

Published: June 27, 2023



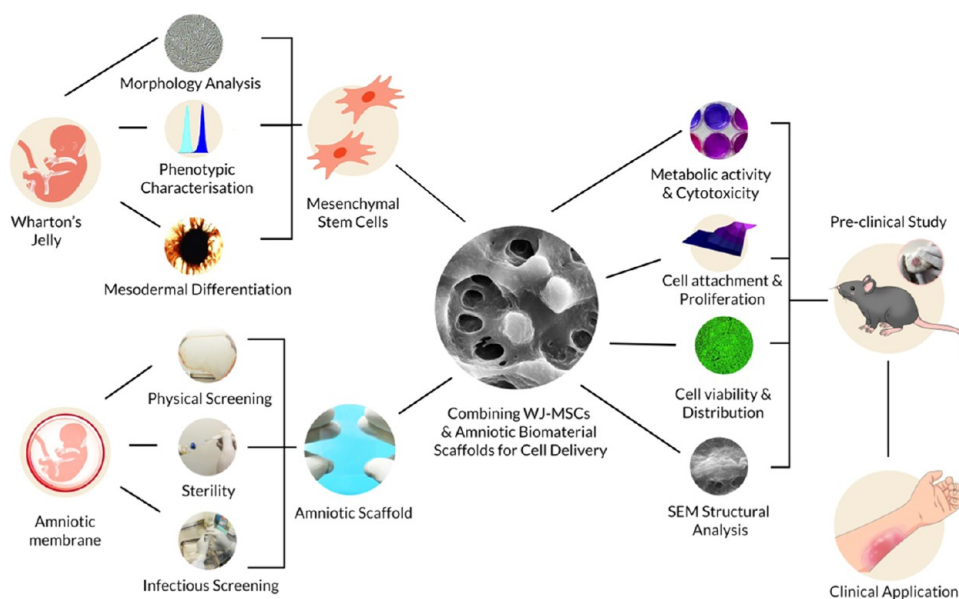


Figure 1. Schematic diagram of combining biological scaffolds seeded with stem cells for cell delivery.

Table 1. Screening Criteria for the Selection of the Amniotic Membrane as a Scaffold

	parameters	method/instrument	specification	results ($n = 5$; AM1–AM5)
physical screening	appearance of tissue	physical observation	maintain the opaque-white appearance	satisfactory
	sign of damage		free of holes/breakage of the membrane	satisfactory
	odor		the tissue free from unacceptable odor	satisfactory
	physical defect		maintains smoothness and elasticity in nature	satisfactory
sterility	contamination		free from debris	satisfactory
	discoloration of tissue		membrane passes the discoloration	satisfactory
	sterility testing (aerobic, anaerobic)	BacT Alert—Biomérieux	negative	negative
infectious diseases screening	endotoxin (LAL assay)	gel clot method—Lonza	<5 EU/mL	negative
	HIV 1 and 2	ELISA method	seronegative	seronegative
	HBsAg	ELISA method	seronegative	seronegative
	anti-HBc	ELISA method	seronegative	seronegative
	CMV—IgM	ELISA method	seronegative	seronegative
	syphilis	PRP method	negative	negative
	malaria	malaria—Ag(ICT)	negative	negative

been employed as a natural scaffold for the healing of different traumas and provides mechanical support for MSC development. Hence, our data reinforce the use of fresh amniotic membranes containing mesenchymal stem cells as an elevator to drive skin formation to some extent.

RESULTS

The schematic outline of the complete process of combining mesenchymal stem cells derived from Wharton's jelly (WJ) and amniotic biomaterial scaffolds for cell delivery is illustrated in Figure 1. In detail, the results of the screening criteria for the selection of the amniotic membrane are tabulated (Table 1) according to the specifications for all samples. In the process, cesarean section placentas are recommended for successful stem cell isolation, since vaginal births may be contaminated and so unsuitable for donation. A Dulbecco's modified Eagle medium–Nutrient mixture of Ham's F-12 with antibiotic and antimycotic is used to keep the retrieved placenta from drying up. Our study's final processed allograft was wafer-like, very

light and thin, accessible, and sutured without tearing. The results of the sterility tests performed were all negative. The basal lamina, which forms a continuous flat and typically smooth layer atop the fibrous collagen stroma, was present and undamaged. The amnion layer's chorion and epithelial cells have been effectively expelled. Also, plainly discernible was the basal lamina. The harvested amnion appeared normal as well; Figure 2 depicts the procedures performed.

The results of the screening criteria for the harvesting of mesenchymal stem cells are tabulated (Table 2) according to the specifications for all of the samples. Wharton's Jelly-derived mesenchymal stem cells (WJMSCs) have been isolated, characterized, and expanded according to a variety of techniques, but they all meet the basic standards recommended by the International Society for Cellular Therapy (ISCT). In this study, we have optimized large-scale expansion of WJMSCs for clinical and therapeutic applications. The cells formed a monolayer of homogeneous spindle-like cells. The cell size underwent no obvious change, as evidenced by the

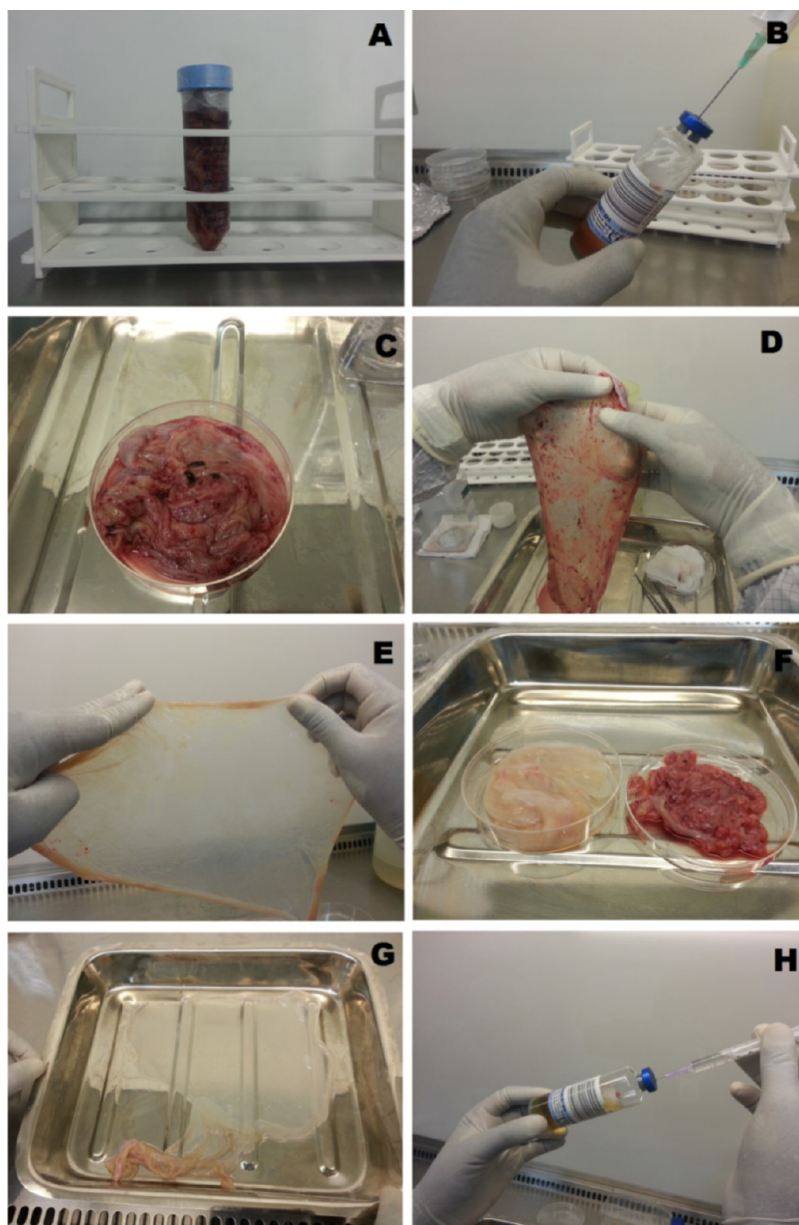


Figure 2. Harvesting of amniotic membrane: (A) amniotic membrane collection and processing within 24 h. (B) Inoculation of a presample in a BACT alert aerobic culture bottle. (C) Amniotic membrane was placed in a Class II Type 2 Biosafety cabinet for blunt dissection processing. (D) Examine the crucial amniotic membrane test parameters for the future procedure (before washing). (E) Processed amniotic membrane cleaned free of blood clots and removed from chorion after being treated with antimicrobial washing solution. (F) Amnion processing and blood clot separation, epithelial layers. (G) Amnion separation from basement layer. (H) Postinoculation of the sample in the BACT alert aerobic culture bottle.

consistent harvested cell density after clinical-scale expansion (Figure 3h,i). In all of the passages, homogeneous reactivity was consistently positive for MSC markers CD73, CD90, and CD105, which are known to be expressed on MSCs, and consistently negative for CD34, CD45, and HLADR. The flow cytometry showed that homogeneous reactivity of consistently more than 90% cells with antibodies was against CD73, CD90, CD105, and less than 1% reactivity was with CD45, CD34, CD79a, and HLADR. This demonstrated that MSCs were phenotype purity and the level of MSC purity was fairly stable between different cell populations (Figure 3g).

Consequently, by using proper medium and growth additives that encourage lineage differentiation, human MSCs have the ability to differentiate into mesodermal lineages. Due of their multipotency, we determined that WJ can develop into

mesodermal cell types such as adipogenic, chondrogenic, and osteogenic cells. By altering the induction media as specified in the **Materials and Methods**, adipogenic, chondrogenic, and osteogenic differentiation procedures were carried out to demonstrate the capacity of WJMSCs to differentiate into diverse mesodermal mesenchymal lineages. Upon 21 days of induction, it was possible to spot tiny fat droplets in the cytoplasm, indicative of adipogenic differentiation. The morphology of the stimulated cells increased and grew with time. Oil red-stained lipid droplets formed in the cytoplasm of positive cells, and the quantity of stained cells increased with time. Figure 3b depicts the developed cells; Figure 3a, the control, does not include any fat droplets. Positive staining of expanded collagen fibers stained with safranin O and chondrocyte pellets (Figure 3d) indicated that MSCs were

Table 2. Screening Criteria for the Harvesting of Mesenchymal Stem Cells

parameters		method/instrument	specification	results ($n = 5$; WJ1–WJ5)
morphology	cell morphology	microscopic observation—Olympus—CKX 31	fibroblast-like spindle-shaped cells in the active growing condition	fibroblast-like spindle-shaped cells in the active growing condition
	viability	tryphan blue—dye exclusion test	>80%	97.02%
sterility	sterility testing (aerobic, anaerobic)	BacT Alert—Biomerieux	negative	negative
	mycoplasma test	mycoAlert—mycoplasma detection assay	negative	negative
	endotoxin (LAL assay)	gel clot method—Lonza	<5 EU/mL	negative
purity	positive markers	flow cytometry—BD FACS caliber	CD73 > 90%	91.78%
			CD90 > 90%	90.23%
			CD105 > 90%	92.53%
	negative markers	flow cytometry—BD FACS caliber	CD34 < 2%	1.87%
			CD45 < 2%	0.31%
			CD79a < 2%	0.17%
infectious diseases screening	HIV 1 and 2	ELISA method	seronegative	seronegative
	HBsAg	ELISA method	seronegative	seronegative
	anti-HBc	ELISA method	seronegative	seronegative
	CMV—IgM	ELISA method	seronegative	seronegative
	syphilis	PRP method	negative	negative
	malaria	malaria—Ag(ICT)	negative	negative

successfully differentiated to chondrocytes with each individual donor sample, and no changes were noticed in undifferentiated or control cells (Figure 3c) to confirm the chondrogenesis potential of WJMSCs.

In an inducing culture media, cells began to undergo morphological changes as early as day 7 for osteogenic differentiation. The cells had a rounder, more cuboidal form instead of their characteristic fibroblastic look. Von Kossa staining was used to determine if WJMSCs could differentiate into osteocytes while being cultivated under osteogenic differentiation circumstances; the strong black staining was seen between osteogenic cells (Figure 3f). In cells cultivated under control conditions, calcium deposition was not seen (Figure 3e). These results indicate that osteoblast-like cells could be generated from WJMSCs by differentiation. The biological properties of MSCs, such as plastic adherence, morphology, specific surface antigens, and multipotent differentiation potential, were retained after clinical-large-scale expansion. Thus, the current study analysis of cell characteristics relates the definition of MSCs.

The cytotoxicity of the biological membrane implanted with WJMSCs was quantified using the 3-(4,5-dimethylthiazol-2-yl)-2,5-diphenyltetrazolium bromide (MTT) test. Cellular death was measured by the release of lactate dehydrogenase (LDH) from the cells on the test samples (TS1 and TS2) after 64 h in the medium corresponded to the number of metabolically active cells. The absorbance values of TS1 and TS2 demonstrated that the MSCs had high vitality and continuous metabolic activity on the biological membrane compared to the positive control (PC) and known sample (cells) controls (KS1–KS4). The outcomes (Figure 4) proved that the metabolic activity of WJMSCs on the scaffold was not inhibited in the medium, and based on the computed scores, it was decided that the biological membrane exhibited no cytotoxic effect.

In the aspect of cell attachment and proliferation, the alamar blue assay is used to determine cellular proliferation. The results depict the percentage decrease of AB with varied

durations and baseline cell densities, as well as the standard curve of percentage (%) AB reduction vs the logarithm of cell growth (Figure 5). Over the whole culture period, the test culture TS2 showed a greater AB decrease than TS1. Similarly, the AB decrease proportion of TS2 was similar to that of KS1 and demonstrated the steady cell growth rate and measured proliferation of MSCs on the scaffold. Over the first 3 days of culture, cell proliferation increased with culture time. By day 5, the metabolic activity of the cells proliferating in the media seemed to diminish, indicating that the surfaces were approaching maximum confluence.

According to a live/dead assay, this hybrid scaffold supports the activity of WJMSCs within a uniform distribution. After day 7 of cell seeding, the viability and spreading of WJMSCs on the amniotic membrane were observed, revealing a large proportion of live cells on the biological membrane. As demonstrated in Figure 6, more than 80% of the cells on the biological scaffold and a significant number of cells on the membrane were alive and uniformly scattered over the membrane, forming a matrix across the layer's surface. The proliferation and dispersion of mesenchymal stem cells increased from day 1 to day 7, and there was no significant change in the viability or morphology as in the fibroblast-like structure after 14 days of culture.

Scanning electron microscopy (SEM) examination of the amniotic membrane exhibited a continuous flat, porous layer of a smooth foundation barrier (Figure 7A). Furthermore, the architecture of MSCs fed for 14 days on an intact amniotic membrane and full confluence development of MSCs (Figure 7B–F) demonstrated the adhesion and proliferation of mesenchymal stem cells on scaffolds.

DISCUSSION

Replete skin injuries and severe dermal burns provide significant issues in dermatology and plastic surgery. They frequently have serious consequences that call for prompt wound closure. However, the paucity of eligible donor sites, poor skin quality, high expenses, and scarring make it difficult

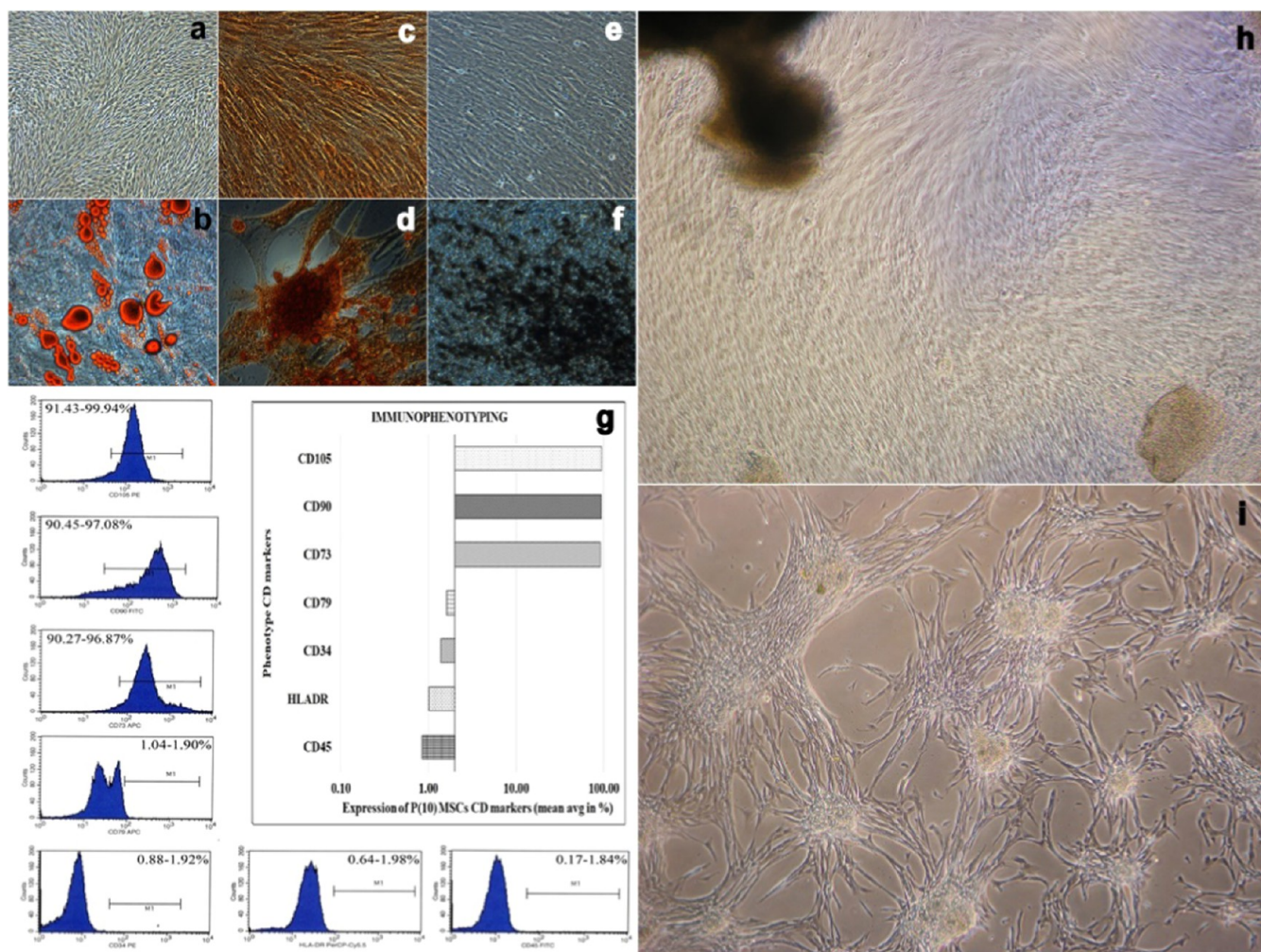


Figure 3. Cell Characterization: adipogenic differentiation potential: (a) adipocontrol and (b) small lipid droplets in the cytoplasm stained with oil red staining. Chondrogenic differentiation potential: (c) chondrocontrol and (d) positive staining of collagen fibers with safranin O stain. Osteogenic differentiation potential: (e) osteocontrol and (f) calcium accumulation was assessed by von Kossa staining. (g) Phenotype analysis when labeled with antibodies against CD34, CD45, HLADR, and CD79a as negative markers and CD73, CD90, and CD105 as specific markers; color-shaded histogram represents positive reactivity with the indicated antibody. (h) WJMSCs form a monolayer of adherent fibroblast-like cells by 48 h: (h) at Passage(0) and (i) at Passage(1), respectively.

to use current treatment methods included as sophisticated dressings and skin transplants.^{14,15} New regenerative techniques including stem cell transplantation, tissue-engineered skin replacements, and bioactive dressing have been proposed to speed up the healing process for wounds. Recent research has shown that using MSCs to treat wounds may have positive effects.^{16,17} Allogeneic MSCs have gained popularity more recently as a source for off-the-shelf goods that are simpler to scale up and commercialize.¹⁸

A novel strategy to improve the effects of cell transplantation is tissue engineering. The viability, proliferation, regenerative effects, and adaptability of the scaffold are improved when stem cells are combined with it. A number of skin abnormalities that are resistant to conventional treatments may be treatable with tissue-engineered products.¹⁵ They generate various cytokines and growth factors that promote collagen production and cell proliferation while reducing pain, inflammation, infection, and scarring. These grafts can also act as a biodegradable scaffold that shields the wound bed from infection while providing a matrix to encourage cell adhesion and proliferation. Additionally, these scaffolds could function

well as a vehicle for delivering and maintaining cells at the transplant site.^{19,20}

The field of regenerative medicine is presently seeing the usage of Wharton's Jelly (WJ) as a biomaterial. Applications for biomaterials are concentrated on cellular growth or cell delivery that can activate cellular responses. To use this biomaterial properly in regenerative medicine, it is required to have a fundamental grasp of Wharton's jelly, decellularization processing technique, and its physical–chemical characteristics. Combining stem cells with biomaterial scaffolds provides a promising strategy for engineering tissues and cellular delivery. In the current study, we optimized the isolation, characterization, and clinical-grade scale up of mesenchymal stem cells and we also standardized the parameters for the amniotic membrane selection for a successful bioscaffold harvesting. We aimed at the assessment of cell metabolic activity, cytotoxicity, attachment, proliferation, viability, distribution, and structural analysis of a tissue-engineered product with a combination of the amniotic membrane as a scaffold seeded with mesenchymal stem cells to prove the potency. All research was carried out in compliance with the

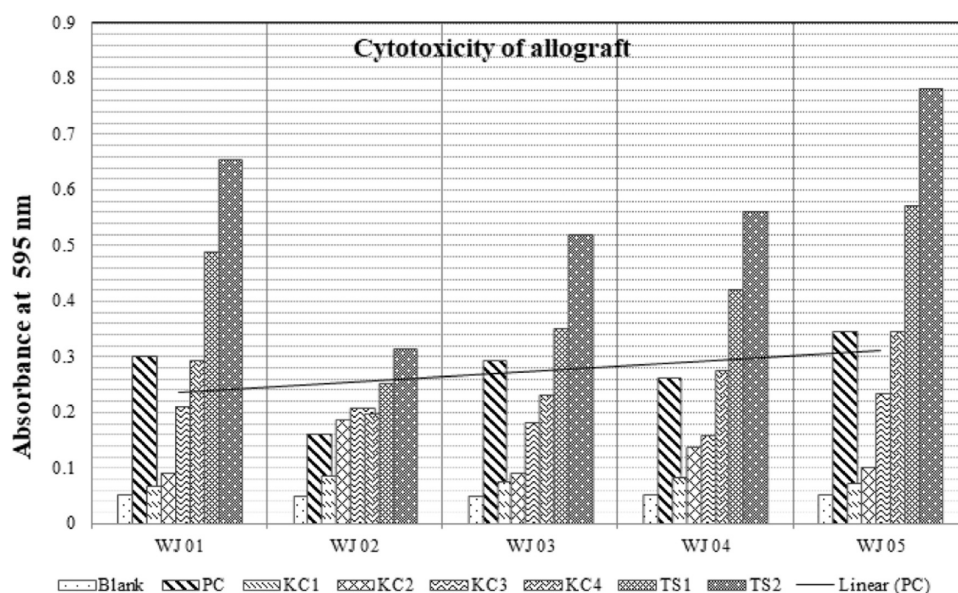


Figure 4. Metabolic activity and cytotoxicity in the scaffold: The cytotoxicity of scaffolds cultivated for 2 weeks was determined using the MTT assay. (Blank) Culture medium without scaffold and cells, (PC) positive control—biological scaffold without cells, (KC1–KC4) known control—25,000, 50,000, 75,000, and 100,000 MSCs seeded without the scaffold, respectively, (TS1 and TS2) test sample—50,000 and 100,000 cells seeded on the scaffold, respectively. (WJ01–WJ05) data represent the mean of five independent experiments.

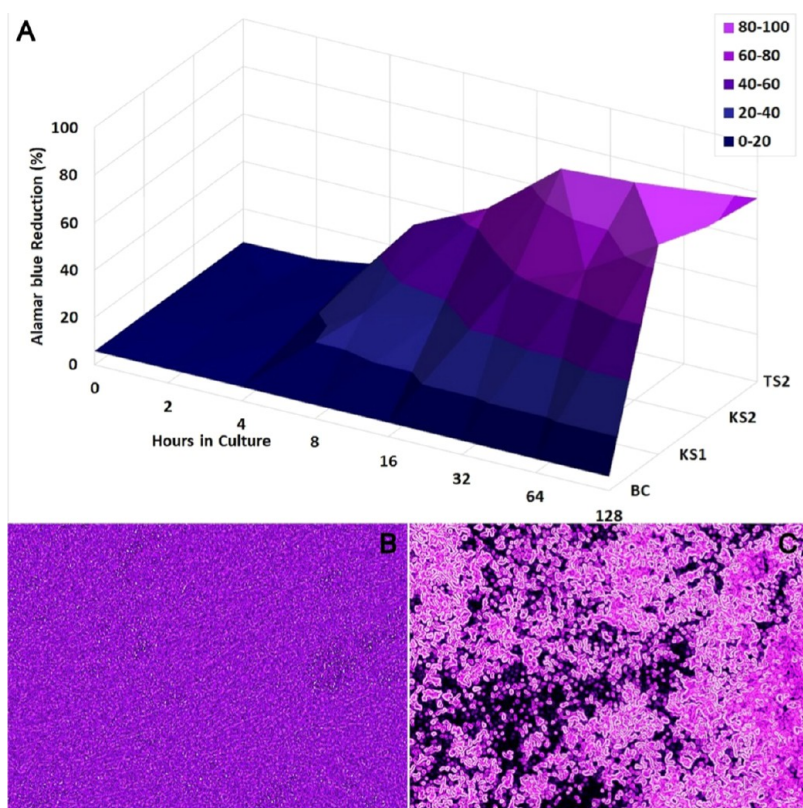


Figure 5. Cell attachment and proliferation: (A) Graph depicting the fraction of AB reduction from blue (oxidized) to pink (reduced) as measured by absorbance at wavelengths of 540 and 630 nm after various durations and cell densities. (B) Microscopic images of AB treated for WJMSC viability/proliferation (KS2). (C) Cells fed on amnion (TS2) for up to 5 days (Magnification 10 \times). Test samples (TS1 and TS2) were 50,000 and 100,000 cells seeded on amnion, respectively, while known sample controls (KS1 and KS2) were 50,000 and 100,000 MSCs planted without amnion. However, the blank control (BC) is culture media without amnion and cells, and the positive control (PC) is amnion without cells.

International Society for Cellular Therapy (ISCT) standards for defining human MSCs. Immuno-phenotype characterization indicated that the MSCs were >90% positive for MSC markers such as CD73, CD90, and CD105. MSCs displayed a

distinctive pattern of cell surface antigens such as CD73, CD90, and CD105. Antigens that are not typically found on MSCs include CD79a, CD34, CD45, and HLADR demonstrating that the isolated MSCs have immuno-phenotype

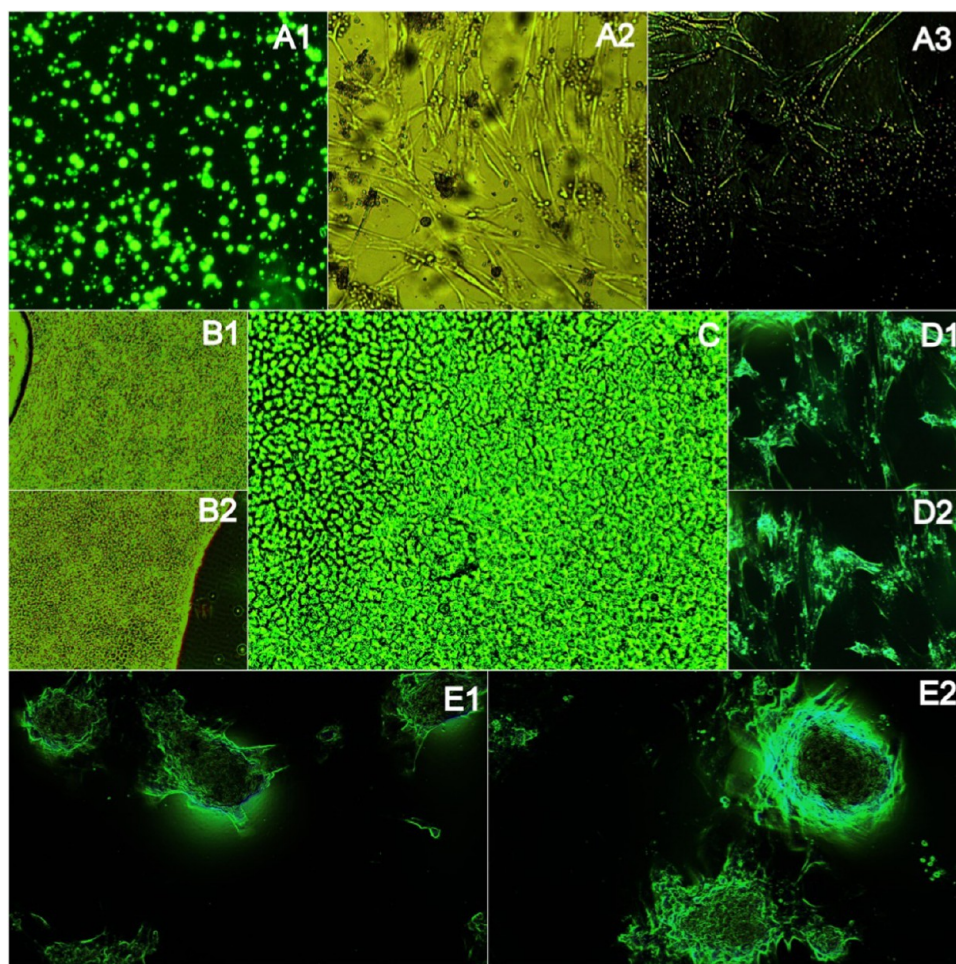


Figure 6. Cell viability and distribution over the allograft: (A1–A3) Cell viability and distribution were determined using fluorescent markers that enabled a live/dead stain, with viable cells labeled green and dead cells marked red (days 1, 7, and 28, respectively). (B1, B2) After 28 and 45 days, observe the amniotic membrane. (C) As a control, a fresh amniotic membrane was used (day 1). (D1, D2) Mesenchymal stem cells adhered, acquired fibroblast shape, and spread throughout the whole amniotic membrane surface. (E1, E2) Live/dead labeling of seeded cells shows that after 14 days, the majority of the cells on the scaffold remain alive (green fluorescence) (magnification 10 \times).

characteristics, capable of self-renewal related to continuous and steady proliferation, and a typical feature of mesenchymal cells. Furthermore, the cells were fibroblast-like and adhered to the plastic culture dish surface, and the results of trilineage differentiation findings revealed that WJMSCs had the potential to develop into osteocytes, adipocytes, and chondrocytes utilizing particular growth conditions.

The potential of WJMSCs to develop into mesodermal lineage is vital for their usage in therapeutics. The current research also demonstrated that biological scaffolds aided in the attachment, proliferation, and differentiation of MSCs. SEM studies revealed that the porous scaffolds' enormous surface area allowed MSCs to attach, disseminate, and develop on it. The flat appearance and good spreading in and around the linked porous structure suggested that cells were adhering and growing strongly.

The long-term viability of WJMSCs seeded on the scaffolds was measured and compared at further time points after seeding. Results show that the amniotic membrane scaffolds have comparable metabolic activity on different intervals after seeding. The bioscaffold showed steady metabolic activity throughout the 14 days, while the monolayer of the cells showed an increase in activity through day 5, after which the activity decreased at day 12. Cellular death results showed a

general increase in cytotoxicity as the metabolic activity of the cells increased, where the metabolic activity peaked. Thus the MSCs seeded and the process of biological scaffold fabrication demonstrated generally good cell survival, indicating that these scaffolds were free of harmful compounds and acceptable for *in vitro* and *in vivo* research.

In terms of cell attachment and proliferation, when MSCs remain functional on the biological scaffold, they maintain a reducing environment in the cell's cytoplasm. Resazurin, the active component in Alamar blue reagent, is a nontoxic, cell-permeable blue chemical that is nearly nonfluorescent. When resazurin enters cells, it is converted into resorufin, a red molecule that is extremely fluorescent. Thus, live MSCs convert resazurin to resorufin constantly, boosting the overall fluorescence and color of the culture fluid around the cells. Thus, this experiment demonstrated that the reducing environment of mesenchymal stem cells on the amniotic membrane, as well as the attraction of alamar blue contained in the reagent, was contributing to the ongoing proliferation of stem cells on the biological scaffold.

The research on the survivability and dispersion of mesenchymal stem cells on biological scaffolds showed that WJMSCs proliferate on the amniotic membrane with obvious distribution and good morphology. The live dead staining

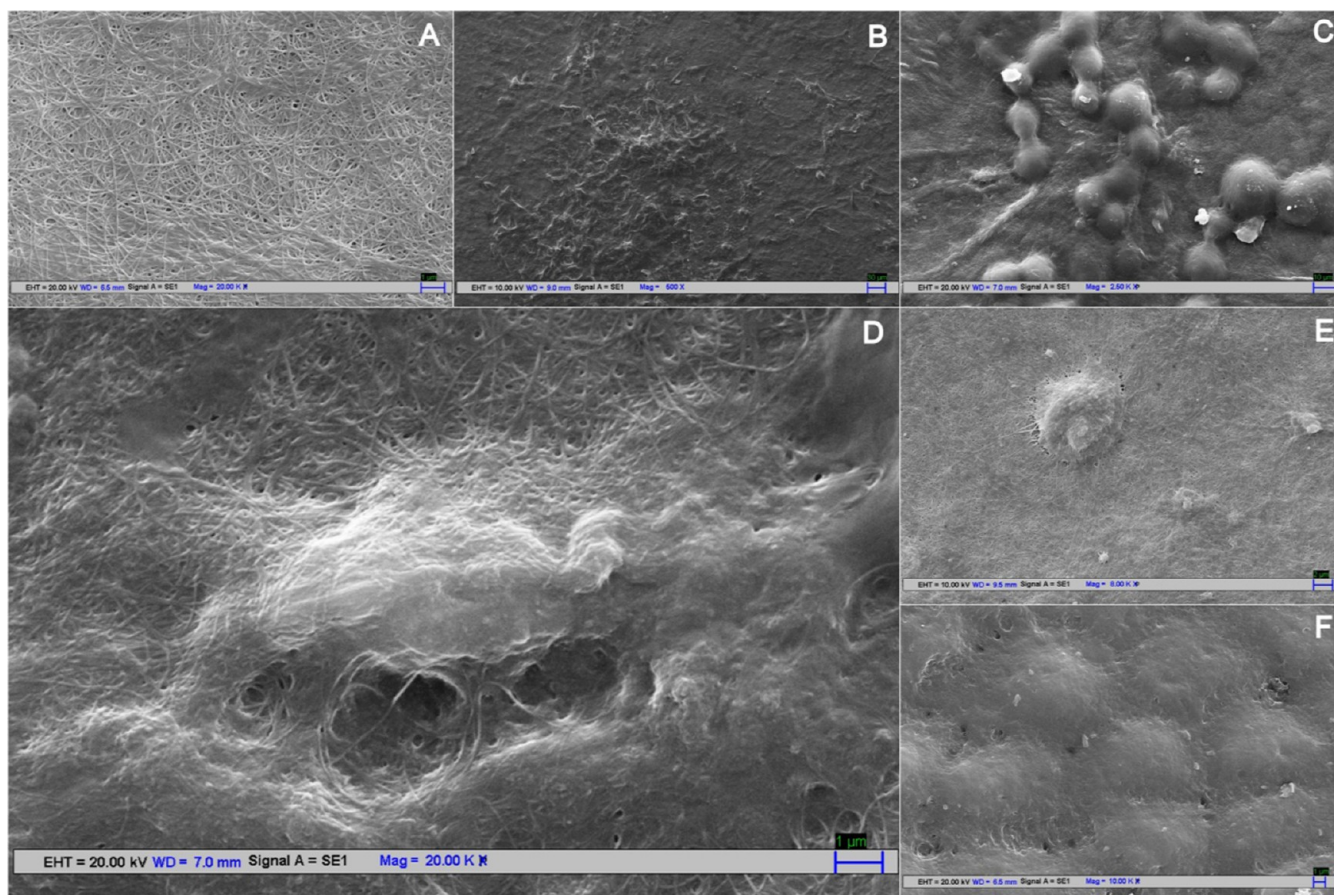


Figure 7. Structural analysis of scaffolds: (A) Morphology of fresh amniotic membrane (magnification 20k \times). (B–F) Morphology of MSCs cultured for 14 days on the fresh amniotic membrane (magnification 500 \times , 2.50k \times , 20k \times , 8k \times , and 10k \times , respectively; scale bar 1 μ m).

demonstrated that more than 80% of the WJMSCs were alive and distributed throughout the biological scaffold. This demonstrates that the good interaction and integration of MSCs with the scaffold and the cells were linked to each other and constructed a cell network over the surface of the membrane, allowing a large number of cells to penetrate and colonize the porous structure.

To accomplish effective healing *in vivo*, the scaffold must be able to offer (i) an appropriate environment for the cells and sufficient porosity to facilitate cell ingrowth without weakening the mechanical properties, (ii) microporosity to present a large surface area for cell–scaffold interactions, and (iii) a biocompatible substance. Importantly, human amniotic membrane and mesenchymal stem cells are readily accessible, and there is no need for a second procedure following transplantation. Taken all together, our research evidenced that the bioscaffold had the most potential as a platform for WJMSCs to improve therapies under the applicable conditions in the field of tissue engineering.

Decellularization or, more specifically, the deepithelialization technique has been used on hAM when examining tissue engineering constructions in further depth. The effectiveness of seeding the three layers—epithelial, basement membrane, and stromal—has been compared by studies mostly in the cartilage tissue engineering region. Cell seeding, proliferation, and differentiation appear to be more advantageous in the basement membrane layer. The decision is primarily influenced by the tissue that needs to regenerate because there is no consensus on the ideal cells to seed on hAM as of

now. In every situation, an appropriate choice must be made between a noninvasive method for the collection of cells and their ultimate functional potential. Furthermore, further research needs to be done on the *in vivo* degradation rate of hAM, which is not sufficiently covered in the literature.

Finally, we note that clinical trials have intensively explored hAM as a scaffold compared to the use of its cells as a tissue engineering construct. Increased knowledge to conduct a preclinical study in order to assess the source of the stem cells, choice of bioactive factors, in particular regarding their function, will encourage future clinical investigations. Eventually, before a clinical application in humans is viable, the *in vitro* optimized tissue engineering approach should be tested in an *in vivo* environment. That is why, another issue to be considered is the most appropriate experimental animal model.

CONCLUSIONS

In our study, we demonstrated the viability of mesenchymal stem cells seeded on the human amniotic membrane using the MTT assay, cell attachment and cellular proliferation using the alamar blue assay, cell distribution over hybrid scaffolds with uniform distribution using the live/dead assay, and the architecture of MSC adhesion and proliferation on scaffolds using SEM. Our findings revealed the viability and proliferative ability of MSCs seeded on hAM. Because of its limitless availability, the practicality of procurement, relative cost-effectiveness, and minimal immunogenicity, AM is in fact a great option for therapeutic applications. Several investigations have delivered evidence of the antifibrotic, anti-inflammatory,

anticancer, antibacterial, wound-healing, and scaffold-like capabilities of AM and a number of research studies backed up the biological features of MSCs; overall, this study shows that depending on the targeted application, hAM has been used as a simple scaffold or seeded with various types of cells that are able to grow and differentiate. Thus, this natural biomaterial seeded with stem cells offers a wide range of applications in tissue engineering.

MATERIALS AND METHODS

Material Source. The investigation was carried out in R&D, CellCure Therapeutics, Coimbatore, India, after prior sanction of the study protocol by the institutional ethical committee. This research was assisted by the Institute for Toxicological Investigations Grant and Biotechnology Industry Research Assistance Council, India.

Procurement of Raw Material. Upon cesarean surgery, the cord of the maternal junction was severed under sterile circumstances, and an amniotic membrane portion of about 12 × 12 cm² was obtained ($n = 5$; AM1–AM5) by manual separation. The separated amniotic membrane and cord tissue were transferred into a sterile 50 mL screw-capped transport medium. For transportation, a medium containing a balanced PBS solution and 15 μL/mL of antibiotic antimycotic solution was used. The collection containers were packed in a collection box and brought to the laboratory at 8–15 °C within 48 h.

Scaffold. Living mothers who gave birth naturally via cesarean section are eligible amnion donors. All amniotic membranes ($n = 5$) were obtained with the donor's written informed consent (participant age range 25–37 year). After that, each donor was asked a series of questions to determine if she had engaged in any actions that might have raised her chance of contracting an infectious disease and whether she had displayed any signs or symptoms of sickness. To eliminate the spread of infectious illnesses from donors to users of the material, donors were prescreened for infectious diseases before being recruited. In the laboratory, the amnion portion was precisely detached from the rest of the chorion, under the Class II Type A2 biosafety cabinet, using blunt dissection and round-ended forceps as per the steps illustrated in Figure 2. Once the detached chorion was removed, the amnion portion was then rinsed thrice with a dissolution medium including a balanced PBS solution as well as 10 μL/mL of the antibiotic antimycotic attempt to eliminate blood and mucus. The amniotic membrane was then maintained for 1 h at room temperature in Dulbecco's modified Eagle medium–Nutrient mixture of Ham's F-12 with the antibiotic solution: 10 μL/mL of antibiotic antimycotic solution.

Cell Isolation and Culture. Mesenchymal stem cells were isolated from the maternal region of the umbilical cord ($n = 5$; WJ1–WJ5) and expanded in the laboratory under the Class II Type A2 biosafety cabinet, and 30–35 jelly explants with a diameter of 0.8 mm were transferred into a tissue-culture-grade T-75 flask containing a culture medium. Nonadherent cells were removed and a new medium was added after incubation at 37 °C for 3–5 days. MSCs were cultured and expanded in Dulbecco's modified Eagle medium–Nutrient mixture of Ham's F-12 (1:1) with Glutamax (1×); 2.438 g/L sodium bicarbonate; sodium pyruvate (DMEM/F12+; Gibco) with 10% PLTMax human platelet lysate (SCM141, Merck) supplemented with 2 ng/mL basic fibroblast growth factor in this study (bFGF; Sigma-Aldrich, U.K.) under standard cell culture conditions (37 °C, 5% CO₂), the and medium was

changed every 3–4 days. In all experimental settings, cells from passage 2 were used with three donors ($N = 3$).

Cell Characterization. WJMSCs were removed from the culture flasks using (TrypLE express), washed with phosphate-buffered saline, and then incubated for 45 min at 4 °C with phycoerythrin (PE)-conjugated antibodies raised against CD34, CD45, CD73, CD90, and CD105 (1:100 dilution) to analyze cell surface markers by flow cytometry. The isotype controls were IgG-PE (all antibodies from BD Pharmingen, NJ). Using BD flow cytometry, the samples were analyzed (FACSCalibur, BD Biosciences).

The methodology outlined by Aurich et al.¹¹ was the basis for the methods, which included several changes. By cultivating WJMSCs for 3 weeks in DMEM/F12+ containing 10% fetal bovine serum (FBS), 108 M dexamethasone (Sigma-Aldrich), 30 g/mL ascorbic acid (Sigma-Aldrich), and 10 mM glycerophosphate (Sigma-Aldrich), the osteoblast differentiation was triggered. New media was supplied every 3 days. Von Kossa staining was used to measure calcium deposition. The differentiated cells were fixed with 10% formalin for 30 min after being rinsed with phosphate-buffered saline. Images were taken using an Olympus CKX41 microscope after the fixed cells were treated with 2.5% sodium thiosulfate for 5 min and 5% silver nitrate for 60 min under UV light (Japan).

To test adipogenic differentiation of WJMSCs, in DMEM/F12+ containing 10% FBS, 1 mM dexamethasone, 0.5 mM isobutyl methyl xanthine, 1 g/mL insulin, and 100 mM indomethacin (Sigma-Aldrich), cells were cultivated for 21 days. Every 3 days, a new inducing component was introduced to the refilled medium. For 20 min, 10% formalin was used to fix the cells. Oil red O staining solution diluted to 200 μL was added, and it was let to sit at room temperature for 10 min. Images were taken using a microscope after five repetitions of distilled water rinsing of the cells.

Chondrogenic differentiation potential was carried out with Invitrogen's STEMPRO chondrogenesis differentiation medium (chondrocyte differentiation basal medium with chondrogenesis supplement) was used to cultivate WJMSCs. Every 3 days, the differentiation media for chondrogenesis was replaced. Cells were fixed with 4% formalin for 30 min before staining. According to the manufacturer's recommendations, Safranin O staining solution was applied and incubated for 5 min. Images were taken using a microscope after the cells had been washed with distilled water.

Cell Seeding of Scaffolds. WJMSCs were expanded to 90% confluence before being passaged and resuspended in Dulbecco's modified Eagle medium–Nutrient mixture of Ham's F-12 (1:1) with Glutamax (1×); 2.438 g/L sodium bicarbonate; and sodium pyruvate (DMEM/F12+; Gibco) with 10% PLTMax human platelet lysate (SCM141, Merck). $5 \times 10^4/10$ and $10 \times 10^4/10$ μL cells were planted dropwise onto an amniotic membrane on a six-well plate and maintained at 37 °C for 3 h to let the cells to adhere prior containing medium to each well. After 3 h, 1 mL of additional medium was added to the scaffolds, which were further cultured under standard conditions.

Cell Seeding Efficiency on Scaffolds. By quantifying the cells adhered to the culture plate an hour after seeding, that is, cells that were not attached to the scaffold, the percentage of cells integrated into the scaffolds was determined. After removing the scaffolds, trypsin–ethylenediaminetetraacetic acid (EDTA) solution was used to separate the residual cells from the well plates so that they could be counted in a

Neubauer chamber. The proportion of cells in the scaffold compared to the total number of cells planted was used to assess the seeding efficiency.

Metabolic Activity and Cytotoxicity in the Scaffold.

64 h after seeding, the metabolic activity of the seeded cells was evaluated by precipitation of the tetrazolium salt. Cellular death was measured by the release of lactate dehydrogenase (LDH) from the cells after 64 h. After incubating the seeded AM for 64 h and removing the medium from the wells, 200 μ L of MTT was applied to 6-well plates and maintained for 4 h at 37 °C in a 5% humidified incubator. Followed by incubation, 1.8 mL of dimethyl sulfoxide (DMSO) was added to dissolve the formazan crystals formed by live cell activity, and the colored supernatant was measured at 490 nm and a reference wavelength of 620 nm with controls including the medium alone (background), cells in well plates without scaffolds (spontaneous LDH release), and cells in well plates without scaffolds with DMSO in the medium (maximum LDH release). The resulting value was then calculated with the equation: cytotoxicity (%) = (experimental value – spontaneous LDH release)/(maximum LDH release – spontaneous LDH release) \times 100.

Cell Attachment and Proliferation. During 2, 4, 8, 16, 32, 64, and 128 h, the cell–scaffold structures were retrieved from the culture plates, rinsed with PBS, and put in 6-well culture plates. With each clone, 2 mL of phenol red removed media containing 10% Alamar blue (R7017, Sigma) was immediately transferred, followed by 24 h incubation at 37 °C in a 5% CO₂ incubator. AB was placed in the medium without cells as a negative control.¹² To determine absorbance, 100 μ L of the solvent was loaded onto 96-well plates and absorbance was measured using an enzyme-linked immunosorbent assay (ELISA) reader at 540 and 630 nm. The number of viable cells was proportional to the extent of dye reduction and was expressed as a proportion of AB decrease. To eliminate phenol red from culture media, the culture media was screened with clean activated charcoal to remove variations caused by medium color. In brief, 17.5 mg of activated charcoal was added per 1 mL media in the culture medium, the container was firmly stirred for 40 min, spun at 1200 RPM for 10 min, and the leftover was filtered to obtain a clear medium.¹³

Cell Viability and Distribution over the Allograft.

After mesenchymal stem cells were dispersed in the fresh amniotic membrane, the cell survival of each allograft was assessed using fluorescence labeling with the live/dead test kit (KS01-100, Biovision). In brief, over several days of incubation, the cell–scaffold constructions (5×10^4 cells/scaffold) were retrieved from the culture plates and rinsed with Hank's balanced salt solution. The allografts were again treated for 60 min at 37 °C with fluorescence diacetate and propidium iodide, rinsed with Hanks' Balanced Salt solution, and assessed under a fluorescence microscope with a band-pass filter (Olympus, Japan). Green fluorescein was used to view healthy living cells, whereas red fluorescein was used to visualize dead cells.

Structural Analysis of Scaffolds. The micro- and macrostructures of the fresh amniotic membrane were analyzed by scanning electron microscopy (SEM) with a range of 2.0 nm at 30 kV (SEM, ZEISS EVO 50). Before SEM examination, specimens were dehydrated with 10–100% ethanol, cured overnight, treated with gold, and then examined under SEM. The numerous capillaries in the amniotic

membrane were quantified precisely from scanning electron microscopy at high magnification (100 \times) from the top view.

■ ASSOCIATED CONTENT

Data Availability Statement

The datasets and all other information are available with the corresponding author and data will be sent by mail upon request.

■ AUTHOR INFORMATION

Corresponding Author

Veeramani Veeramani – PG and Research Centre in Microbiology, MGR College, Hosur 635130 Tamil Nadu, India; orcid.org/0000-0002-6235-1223;
Email: vra.manikandan@gmail.com

Authors

Umamagesh Palaniappan – PG and Research Centre in Microbiology, MGR College, Hosur 635130 Tamil Nadu, India; Department of Microbiology, Sri Kailash Women's College, Periyeri, Thalavasaal, Attur 636 112 Tamil Nadu, India

Jaianand Kannaiyan – Research and Development, CellCure Therapeutics, Coimbatore 625014 Tamil Nadu, India; Research and Development, Bogar BioBee Stores Pvt. Ltd, Coimbatore 641046 Tamil Nadu, India

Balaji Paulraj – PG and Research Centre in Biotechnology, MGR College, Hosur 635130 Tamil Nadu, India

Ponmurugan Karupiah – Department of Botany and Microbiology, College of Science, King Saud University, Riyadh 11451, Saudi Arabia

Santhosh Basavarajappa – Department of Dental Health, Dental Biomaterials Research Chair, College of Applied Medical Sciences, King Saud University, Riyadh 11433, Saudi Arabia

Asad Syed – Department of Botany and Microbiology, College of Science, King Saud University, Riyadh 11451, Saudi Arabia

Abdallah M. Elgorban – Department of Botany and Microbiology, College of Science, King Saud University, Riyadh 11451, Saudi Arabia

Noof S. Zaghoul – Bristol Centre for Functional Nanomaterials, HH Wills Physics Laboratory, University of Bristol, Bristol BS8 1FD, U.K.

Complete contact information is available at:

<https://pubs.acs.org/10.1021/acsomega.3c01689>

Author Contributions

Conceptualization and resources, J.K. and V.V.; methodology, J.K. and U.P.; software, R.E. and U.P.; validation, A.M.E., J.K., and S.B.; data curation, A.S., R.K.K., and U.P.; writing—original draft preparation, J.K.; writing—review and editing, O.R.A., N.S.Z., M.A.A., and P.K.; supervision and funding acquisition, V.V.; project administration, B.P. All of the authors have read and agreed to the published version of the manuscript.

Notes

The authors declare no competing financial interest.

The animal study protocol was approved by the Institutional Animal Ethics Committee of Nandha College of Pharmacy, Erode, Tamil Nadu, India (NCP/IAEC/2018-19/11), for studies involving mesenchymal stem cells.

ACKNOWLEDGMENTS

The authors thank CellCure Therapeutics for the institutional research board (NCP/IAEC/2018-19/11), and Nandha College of Pharmacy, Erode, for the study support, as per the guidelines of the Institutional Animal Ethical Committee 9688/PO/Re/S/02/CPCSEA. This work was partially funded by the researchers supporting Project Number CCT-2019/43, CellCure Therapeutics, and Researchers Supporting Project number (RSP2023RS56), King Saud University, Riyadh, Saudi Arabia.

REFERENCES

- (1) Zhang, Y.; Wu, D.; Zhao, X.; et al. Stem Cell-Friendly Scaffold Biomaterials: Applications for Bone Tissue Engineering and Regenerative Medicine. *Front. Bioeng. Biotechnol.* **2020**, *8*, No. 598607.
- (2) Alaribe, F. N.; Manoto, S.; Motaung, S. Scaffolds from biomaterials: Advantages and limitations in bone and tissue engineering. *Biologia* **2016**, *71*, 56.
- (3) Kong, L.; Gao, Y.; Lu, G.; Gong, Y.; Zhao, N.; Zhang, X. A study on the bioactivity of chitosan/nano-hydroxyapatite composite scaffolds for bone tissue engineering. *Eur. Polym. J.* **2006**, *42*, 3171–3179.
- (4) Rodríguez-Vázquez, M.; Vega-Ruiz, B.; Ramos-Zúñiga, R.; Saldaña-Koppel, D. A.; Quiñones-Olvera, L. F. Chitosan and Its Potential Use as a Scaffold for Tissue Engineering in Regenerative Medicine. *Biomed. Res. Int.* **2015**, *2015*, No. 821279.
- (5) Kannaiyan, D. J.; Hemlata, C.; Palaniyandi, M.; Rajangam, B.; Suriya, S.; Anubhav, P. Biological and synthetic scaffold: an extra cellular matrix for constructive tissue engineering. *Int. J. Med. Res. Rev.* **2016**, *4*, 1882–1896.
- (6) Malhotra, C.; Jain, A. K. Human amniotic membrane transplantation: Different modalities of its use in ophthalmology. *World J. Transplant.* **2014**, *4*, 111–121.
- (7) Jaianand, K.; Saurabh, K.; Suriya, N.; Firdosh, M. Dehydrated Amniotic Allograft Seeded with Stem Cells: the clinical Perspectives for Wound Healing. *J. Stem. Cell Regen. Biol.* **2019**, *5*, 16–24.
- (8) Hmadcha, A.; Martin-Montalvo, A.; Gauthier, B. R.; Soria, B.; Capilla-Gonzalez, V. Therapeutic Potential of Mesenchymal Stem Cells for Cancer Therapy. *Front. Bioeng. Biotechnol.* **2020**, *8*, 43.
- (9) Levy, O.; Kuai, R.; Siren, E. M. J.; et al. Shattering barriers toward clinically meaningful MSC therapies. *Sci. Adv.* **2020**, *6*, No. eaba6884.
- (10) Margiana, R.; Markov, A.; Zekiy, A. O.; et al. Clinical application of mesenchymal stem cell in regenerative medicine: a narrative review. *Stem Cell Res. Ther.* **2022**, *13*, 366.
- (11) Aurich, I.; Mueller, L. P.; Aurich, H.; et al. Functional integration of hepatocytes derived from human mesenchymal stem cells into mouse livers. *Gut* **2007**, *56*, 405–415.
- (12) Al-Nasiry, S.; Geusens, N.; Hanssens, M.; et al. The use of Alamar Blue assay for quantitative analysis of viability, migration and invasion of choriocarcinoma cells. *Hum. Reprod.* **2007**, *22*, 1304–1309.
- (13) Nociari, M. M.; Shalev, A.; Benias, P.; Russo, C. A novel one-step, highly sensitive fluorometric assay to evaluate cell-mediated cytotoxicity. *J. Immunol. Methods* **1998**, *213*, 157–167.
- (14) Lei, Z.; Singh, G.; Min, Z.; Shixuan, C.; Xu, K.; Pengcheng, X.; et al. Bone marrow-derived mesenchymal stem cells laden novel thermo-sensitive hydrogel for the management of severe skin wound healing. *Mater. Sci. Eng., C* **2018**, *90*, 159–167.
- (15) Goodarzi, P.; Alavi-Moghadam, S.; Sarvari, M.; et al. Adipose tissue-derived stromal cells for wound healing. *Adv. Exp. Med. Biol.* **2018**, *1119*, 133–149.
- (16) Isakson, M.; De Blacam, C.; Whelan, D.; McArdle, A.; Clover, A. Mesenchymal stem cells and cutaneous wound healing: current evidence and future potential. *Stem Cells Int.* **2015**, *2015*, No. 831095.
- (17) Abd-Allah, S. H.; El-Shal, A. S.; Shalaby, S. M.; Abd-Elbary, E.; Mazen, N. F.; Abdel Kader, R. R. The role of placenta-derived mesenchymal stem cells in healing of induced full-thickness skin wound in a mouse model. *IUBMB Life* **2015**, *67*, 701–709.
- (18) Sterodimas, A.; de Faria, J.; Nicaretta, B.; Pitanguy, I. Tissue engineering with adipose-derived stem cells (ADSCs): current and future applications. *J. Plast. Reconstr. Aesthet. Surg.* **2010**, *63*, 1886–1892.
- (19) Miyazaki, H.; Tsunoi, Y.; Akagi, T.; Sato, S.; Akashi, M.; Saitoh, D. A novel strategy to engineer pre-vascularized 3-dimensional skin substitutes to achieve efficient, functional engraftment. *Sci. Rep.* **2019**, *9*, No. 7797.
- (20) Kallis, P. J.; Friedma, A. J.; Lev-Tov, H. A guide to tissue-engineered skin substitutes. *J. Drugs Dermatol.* **2018**, *17*, 57–64.